Developmental Biology 357 (2011) 83–95

Contents lists available at ScienceDirect

Developmental Biology

journal homepage: www.elsevier.com/developmentalbiology

Evolution of Developmental Control Mechanisms

Evolution of *nubbin* function in hemimetabolous and holometabolous insect appendages

Nataliya Turchyn [a], John Chesebro [b], Steven Hrycaj [a], Juan P. Couso [b], Aleksandar Popadić [a,*]

[a] Department of Biological Sciences, Wayne State University, Detroit, MI 48202, USA
[b] School of Life Sciences, University of Sussex, Brighton BN1 9QG, UK

ARTICLE INFO

Article history:
Received for publication 22 November 2010
Revised 10 June 2011
Accepted 11 June 2011
Available online 25 June 2011

Keywords:
Acheta domesticus
Periplaneta americana
nubbin (*nub*)
Leg segmentation
Coxa
Trochanter
Tibia
Tarsus

ABSTRACT

Insects display a whole spectrum of morphological diversity, which is especially noticeable in the organization of their appendages. A recent study in a hemipteran, *Oncopeltus fasciatus* (milkweed bug), showed that *nubbin (nub)* affects antenna morphogenesis, labial patterning, the length of the femoral segment in legs, and the formation of a limbless abdomen. To further determine the role of this gene in the evolution of insect morphology, we analyzed its functions in two additional hemimetabolous species, *Acheta domesticus* (house cricket) and *Periplaneta americana* (cockroach), and re-examined its role in *Drosophila melanogaster* (fruit fly). While both *Acheta* and *Periplaneta nub*-RNAi first nymphs develop crooked antennae, no visible changes are observed in the morphologies of their mouthparts and abdomen. Instead, the main effect is seen in legs. The joint between the tibia and first tarsomere (Ta-1) is lost in *Acheta*, which in turn, causes a fusion of these two segments and creates a chimeric *nub*-RNAi tibia–tarsus that retains a tibial identity in its proximal half and acquires a Ta-1 identity in its distal half. Similarly, our re-analysis of *nub* function in *Drosophila* reveals that legs lack all true joints and the fly tibia also exhibits a fused tibia and tarsus. Finally, we observe a similar phenotype in *Periplaneta* except that it encompasses different joints (coxa–trochanter and femur–tibia), and in this species we also show that *nub* expression in the legs is regulated by Notch signaling, as had previously been reported in flies and spiders. Overall, we propose that *nub* acts downstream of Notch on the distal part of insect leg segments to promote their development and growth, which in turn is required for joint formation. Our data represent the first functional evidence defining a role for *nub* in leg segmentation and highlight the varying degrees of its involvement in this process across insects.

Introduction

Insect appendages are immensely diverse and serve as a rich source for studying morphological evolution. In general terms, serially homologous appendages that originate from different segments exhibit the most obvious differences. For example, appendages such as fore and hind wings or mouthparts such as mandibles, maxillae, and labium are all characterized by distinct phenotypes. Based on a large body of evidence, from classic experiments in *Drosophila* to more recent studies in *Tribolium*, *Bombyx*, *Oncopeltus*, *Gryllus,* and *Acheta,* it is now well documented that these serial differences are mainly regulated by Hox genes (Abzhanov and Kaufman, 2000; Brown et al., 2000; Chesebro et al., 2009; Lewis, 1978; Lewis et al., 2000; Mahfooz et al., 2007; Masumoto et al., 2009; Rogers et al., 2002; Tomoyasu et al., 2005; Zhang et al., 2005). However, while much is understood regarding the genetic mechanisms that govern individual appendage identity, much less is known about the molecular basis of variation that exists within each appendage type. Thus, the genetic origins of many species-specific morphologies, such as the pigmentation, shape, and size of a fore wing or a fore leg remain largely unknown. A number of recent studies have provided support to the idea that developmental variation may be the leading cause of the large amount of phenotypic diversity observed between the appendages of even closely related species (Averof and Patel, 1997; Gompel et al., 2005; Mahfooz et al., 2007; Rogers et al., 2002; Tomoyasu et al., 2009; Wittkopp et al., 2002). In order to better understand this putative relationship between developmental and phenotypic variation, we chose to further investigate the functional role of the POU homeodomain gene *nubbin* (*nub*) in *Acheta* and *Periplaneta*, two basal hemimetabolous insect lineages.

Previous work has revealed that *nub* is an important developmental gene whose expression has been shown to be highly dynamic and variable throughout the appendages in several arthropod lineages (Abzhanov and Kaufman, 2000; Damen et al., 2002; Li and Popadić, 2004; Prpic and Damen, 2009). In *Drosophila melanogaster, nub* is expressed in the central nervous system (CNS), wing pouch and hinge (Billin et al., 1991; Cifuentes and Garcia-Bellido, 1997; Ng et al., 1995), and in regions along the developing leg near the future position of

* Corresponding author. Fax: +1 313 577 6891.
E-mail address: apopadic@biology.biosci.wayne.edu (A. Popadić).

0012-1606/$ – see front matter © 2011 Elsevier Inc. All rights reserved.
doi:10.1016/j.ydbio.2011.06.014

joints (Mirth and Akam, 2002; Rauskolb and Irvine, 1999). In another holometabolous species, *Bombyx mori* (silkworm), *nub* expression encompasses the entire wing disc (Kango-Singh et al., 2001). Recently, *nub* expression was evaluated in two basal insect lineages, *Thermobia* (firebrat) and *Periplanata* (cockroach), and in a moderately derived hemimetabolous species, *Oncopeltus* (milkweed bug) (Li and Popadić, 2004). In all three insects, *nub* displays a distinct, species-specific pattern in the head appendages and legs. In addition, a novel domain was observed in a posterior region of *Oncopeltus* embryos that corresponds to part of the future abdomen (Hrycaj et al., 2008). These results highlight a wide range of diversity in *nub* expression in insects and suggest that its level of functional divergence may be equally high.

To date, the function of *nub* in insects has only been described in *Drosophila* and *Oncopeltus*. In flies, *nub* is recognized for its role in growth and proximal–distal patterning of wings (Cifuentes and Garcia-Bellido, 1997; Neumann and Cohen, 1998; Ng et al., 1995), and maturation of neuroblast cells (Bhat and Schedl, 1994). Aside from the brief reference to causing "shortened and gnarled" legs in *nub* hypomorphic mutants, *nub* function in fly leg development is undocumented (Cifuentes and Garcia-Bellido, 1997). In *Oncopeltus*, however, *nub* is necessary for proper development of the antennae and labium in the head and for the growth of the femoral segment in all three pairs of legs (Hrycaj et al., 2008). It also has a novel function in the abdomen where it represses limb formation by controlling the Hox gene *abd-A*. To determine whether, and to what degree, these roles are conserved in other insects, we performed a detailed analysis of *nub* expression and function in *Acheta*. In addition, we extended our previous expression studies in *Periplaneta* (Li and Popadić, 2004) by performing functional analysis and reassessed the role of *nub* in *Drosophila* leg development. Our study shows that *Acheta nub* mRNA accumulates in the head appendages, legs, and abdomen in a pattern that is different from *Oncopeltus* and highlights the presumptive leg joints. Subsequent maternal RNA interference (RNAi) experiments show that while *nub*-depleted first nymphs exhibit crooked antennae, their gnathal appendages (mandibles, maxillae, and labium) are unaffected. Interestingly, *nub* does not have any discernable role in the abdomen, despite its expression in this region. The most prominent feature of *nub* RNAi phenotype is observed in the thorax, where all three pairs of legs are severely undersized due to reduced trochanter (Tr) and femur (Fe), and to fusion between the tibia (Ti) and first tarsomere (Ta-1). *Periplaneta nub* expression also accumulates in legs near the presumptive joints and *nub*-depleted cockroaches exhibit an *Acheta*-like phenotype of fused segments (Cx/Tr and Fe/Ti). Our analysis of *Drosophila nub* null mutants reveals fusions between leg segments, as well as the loss of claws and all joints, except some between tarsal sub-segments. To our knowledge, these results constitute the first functional evidence of the involvement of *nub* in insect leg segment development and demonstrate the varying degrees of plasticity in its contribution to joint formation.

Materials and methods

Insect cultures

A. domesticus were raised at room temperature on a diet of fresh lettuce leaves supplemented by dry cat food and water. The laid eggs were collected on a daily basis and incubated at 30 °C in a moist environment for all experiments.

P. americana were originally purchased from Carolina Biological Supply Company (Burlington, USA) and were maintained in the laboratory under conditions previously described in Hrycaj et al. (2010). The laid oothecae (egg cases) were handled in the same way as *Acheta* eggs.

Drosophila nub null individuals used in this study were generated and described by Hrycaj et al. (2008). Briefly, nub^{E37}/*CyO-ftzlacZ* flies were crossed to either *Df(2L)GR4/CyO* or *Df(2L)prd1.7/CyO* (Bloomington Stock Centre). The *nub* mutant class was identified as pharate adults by virtue of its number and wing phenotype. The *odd-lacZ* line was donated by T. Kline (Dusseldorf, Germany) and both live pharates and freshly emerged imagos were dissected and stained to reveal ß-gal activity as described in Couso et al. (1994). The *pdm2* mutants used were $pdm2^{\{XP\}d09994}$ (Bloomington Stock Centre).

Generation of Acheta nub cDNA

The total RNA isolation and synthesis of cDNA, RT-PCR, and cloning were carried out according to the previously described protocols (Li and Popadić, 2004). Briefly, degenerate primers targeting the highly conserved amino acid motifs EQFAKT (5′-GGAATTCGARCARTT YGCIAARAC-3′) and KEKRINP (5′-GCTCTAGAGGRTTIATICKYTTY-CYTT-3′) were used to generate a 387 bp long PCR fragment of *Acheta nub* that was then cloned into a pCR4-TOPO vector and verified by sequencing (GenBank sequence accession number HQ543076). The nucleotide sequences from ten clones were compared with each other and to other previously described *nub* orthologs. No evidence of paralogous copies was found.

In situ hybridization and immunostaining

The synthesis of digoxigenin-labeled antisense *nubbin* RNA probes and in situ hybridization procedure were performed as described in Li and Popadić (2004). *Ubx* expression was detected using the mouse monoclonal antibody FP 6.87 (1:8; donated by R. White) according to the protocol by Mahfooz et al. (2004). Zeiss Axiophot and Leica TCS SP2 laser confocal scanning microscopes were used to take images of in situ hybridization- and antibody-stained embryos, respectively.

For *Drosophila* antibody staining, pupae were collected and staged from the *odd-lacZ* stock, dissected, and stained as described in Galindo et al. (2005). The antibodies used were: anti-Nub (1:10; donated by S. Cohen) and anti-ßgal (1:1000; Sigma, St. Louis, MO, USA, catalog #94644).

RNA interference (RNAi)

To analyze *nub* function, we injected adult *Acheta* females with *nub* double-stranded RNA (dsRNA) of two different lengths according to the maternal RNAi methodology described in Mahfooz et al. (2007). Both *nub* dsRNA transcripts generated essentially the same RNAi phenotypes. Specifically, 6 µl of *nub* dsRNA at a concentration of 2.5 µg/µl was injected into the abdomens of female crickets using a Hamilton syringe with a 32-gauge needle. Following injections, they were placed in separate containers and reared with wild type males. The eggs were collected daily and incubated at 30 °C. Some of them were left undisturbed, while those intended for in situ and antibody staining were dissected at various stages of development. Both the embryos that died before completing embryogenesis (approximately 95% development) and those that emerged into first nymphs were scored for *nub* RNAi phenotypes. We examined a total of 1061 embryos and first nymphs and placed them into two different classes depending on the phenotypic severity (class I — strong and class II — moderate). For double RNAi experiments, *Acheta* females were injected with equimolar amounts of *nub* and *Ubx* dsRNA that was previously generated by Mahfooz et al. (2007). To control for nonspecific side effects of RNAi, we analyzed the progeny of crickets injected with a 375 bp fragment of GFP dsRNA. All GFP-treated embryos and first nymphs were indistinguishable from wild type controls.

To generate RNAi phenotypes in *Periplaneta*, nine fertilized adult females were injected with *nub* dsRNA according to the methodology

described in Hrycaj et al. (2010). Briefly, a total of 567 embryos and first nymphs were examined with 266 displaying wild type phenotype and 301 exhibiting morphological changes of different severity.

RT-PCR analysis

Total RNA isolation and synthesis of cDNA were carried out as described previously (Hrycaj et al., 2010; Li and Popadić, 2004). Total RNA was extracted from whole embryos exhibiting RNAi phenotypes using Trizol (GibcoBRL/Life Technologies). This RNA was then used to produce cDNA utilizing poly-T primer (Promega). In the same way, we generated total RNA and cDNA from corresponding stages of wild type embryos. RT-PCR was performed according to Hrycaj et al. (2010) by using unique sets of primers that were designed to amplify shorter *Acheta* and *Periplaneta nub* fragments. In addition, universal 18S (QuantumRNA™ 18S Internal Standards, Ambion, Austin, TX, USA) primers with competimer (3:7 ratio) were used to generate ribosomal protein 18S that served as the internal control. The PCR conditions were as followed: denaturation at 95 °C for 2 min, annealing at 58.3 °C (*Acheta*) and 51.3 °C (*Periplaneta*) for 30 s, and extension at 72 °C for 30 s for 33 (*Acheta*) and 34 (*Periplaneta*) cycles.

Leg measurements and data analysis

The images of the dissected mid (T2) and hind (T3) legs from sixteen *Acheta* first nymphs were taken with a SPOT RT CCD digital camera (Diagnostic Instruments) connected to a LEICA MZ 12.5 microscope. The total leg length, as well as the length of individual leg segments (femur, tibia, and tarsus), was measured along the proximal–distal axes by using a SPOT 4.5 software. Each leg and its segments were measured twice and the variance between the repeated measurements was analyzed using ANOVA (SPSS Version 11.5). Because there was no significant difference between the two measurements, we averaged them and utilized these data for final ANOVA analysis.

Results

Embryonic expression patterns of Acheta nub

At 22% development, *nub* mRNA is expressed in all head appendages and thoracic leg buds at varying levels of intensity (Fig. 1A). In the head region, while a strong signal is observed in the antennae, only weak expression is detected in the distal-most tip of the mandibles. *nub* is also present throughout the maxillary and labial limb buds, with a higher level of intensity being restricted to their distal ends (Fig. 1A′, inset). In the thorax, a strong accumulation of *nub* is observed in the mid-distal portions of all leg buds (Fig. 1D). At this stage, no signal is present in the abdomen except in its posterior-most segment (Fig. 1A). At 27% development, the initial *nub* domain in the legs resolves into a series of rings (Fig. 1E). Slightly later (30% development), the *nub* expression in the antennae differentiates into three concentric bands (labeled as 1, 2, and 3) in the proximal–distal direction (Figs. 1B and B′, inset). At this stage, *nub* signal now encompasses the entire mandibles and its level also increases in both maxillary and labial appendages. In the legs, the existing two rings expand and split (Fig. 1F). In the abdomen, *nub* is now detected in the region corresponding to the presumptive proctodeum (Fig. 1B). As shown in Fig. 1G, at 40% development, leg domain II divides into two distinct rings (II_A and II_B).

By 50% development, a new domain (band 4) and a diffused patch (marked with asterisk) of *nub* appear in the distal region of the antennae (Figs. 1C and C′, inset). The signal still accumulates throughout the mandibles with a higher level of expression being restricted to their distal-most parts. At this stage, *nub* expression in the maxillary and labial appendages resolves into two rings (labeled as a and b) in the proximal-mid region and a "sock" distal to it (Fig. 1C′, inset). In the legs, domain I is further divided in two narrow bands (I_A and I_B) that are much weaker compared to signal in II_A and II_B (Fig. 1H). In the abdomen, *nub* expression is still visible in the developing proctodeum (Fig. 1C). As *Acheta* embryogenesis proceeds, *nub* accumulation disappears from all head appendages, while in the legs only rings II_A and II_B remain, corresponding to distal femur and distal tibia (Fig. 1I).

Acheta nub RNAi first nymphs are characterized by crooked antennae and significantly shortened thoracic legs

To examine the functional significance of *nub* expression patterns, we utilized the previously described maternal RNAi approaches (Hrycaj et al., 2008; Mahfooz et al., 2007). The administration of *nub* dsRNA effectively suppresses the accumulation of *nub* transcript in developing *Acheta* embryos (Figs. 2I and K). We analyzed a total of 1061 embryos and first nymphs of whom 43.7% are wild type and 56.3% exhibit distinct morphological changes. Similar to *Drosophila* mutants (Bhat and Schedl, 1994) and *Oncopeltus* RNAi embryos (Hrycaj et al., 2008), a large percentage (57.8%) of individuals displaying *nub* RNAi phenotypes do not hatch, although they complete approximately 95% of development. The remaining embryos are capable of hatching into first nymphs but die shortly after. Overall, *nub* RNAi phenotypes display morphological changes that range from strong (class I) to moderate (class II). Class I includes embryos and first nymphs that exhibit severe alterations of the antennae and all three pairs of legs. Class II individuals, on the other hand, show changes mainly in the hind legs. In addition, few of them have antennae similar to ones observed in class I.

In the present study, we focused on class I first nymphs rather than embryos because the mutant phenotypes observed in the former can be exactly compared to the corresponding stage in wild type, allowing us to accurately measure their legs. The abolition of *Acheta nub* causes morphological changes in two body regions: the head and thorax (Fig. 2B). In the head, the mid-distal part of the antenna becomes crooked due to the fusion of adjacent segments (Figs. 2C and C″, inset). Note that although *nub* mRNA accumulates in all gnathal appendages (maxillae, labium, and mandibles), we do not observe any changes in their external morphologies (Figs. 2D1–D3).

Wild type first nymphs have greatly enlarged hind (T3) legs when compared to their fore leg (T1/T2) counterparts (Fig. 2E). In T2 legs, the tibia and tarsus appear similar in length and are only slightly longer than the femur. In "jumping" hind legs, however, the femur is by far the largest segment (podomere), followed by the tibia, and then the tarsus. Note that the tarsus of all legs is divided into three subunits called tarsomeres (Figs. 2E′ and E″, insets). The first tarsomere (Ta-1) is always the longest, followed by Ta-3, while the second tarsal subunit (Ta-2) is the smallest. *nub* RNAi hatchlings exhibit three major defects in their legs. First, their overall length is visibly reduced mainly by a shortening of the tibia and tarsus, and to a much lesser degree, the femur (Figs. 2E and F). Second, there is a decrease in the size of the trochanter (compare Figs. 2E′ vs. F′, insets). Third, *nub* RNAi legs appear to lack a distinct proximal-most tarsomere (Ta-1), while the second and third tarsal subunits are slightly affected in size but not in morphology (Figs. 2F′ and F″, insets). Thus, these findings reveal that in *Acheta, nub* is necessary for both the formation of Ta-1 and for leg elongation.

To determine the degree of actual leg shortening, we measured the total leg length as well as the length of individual segments (femur, tibia, and tarsus) in wild type and *nub*-depleted first nymphs (Figs. 2G and H). In the former, the overall length of the T2 and T3 legs are 1432 μm and 2423 μm, respectively (Fig. 2G, solid bars). The depletion of *nub* causes hatchlings to develop significantly shorter T2 legs (1040 μm long), demonstrating a 27.3% reduction (Fig. 2G, striped

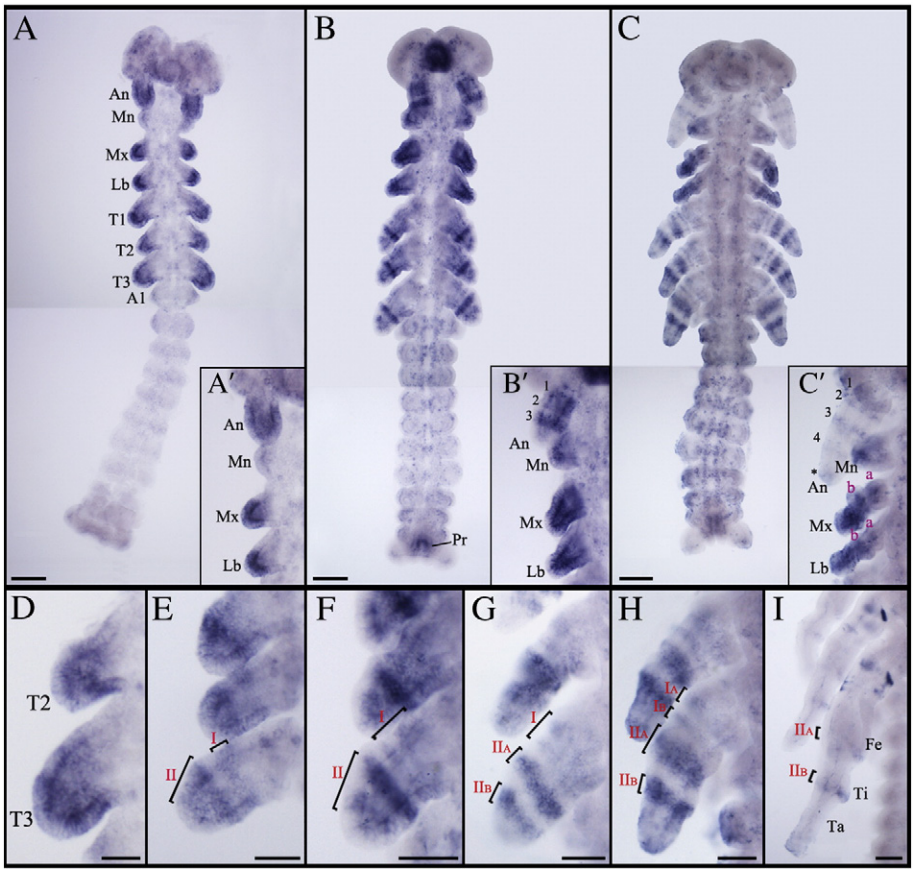

Fig. 1. Expression patterns of *nub* mRNA in wild type *Acheta* embryos. (A) At 22% development, *nub* transcript accumulates in all head appendages and thoracic limb buds with varying levels of intensity and in the posterior-most edge of the abdomen. (A′, inset) Close-up view of the head region at this stage shows that while antennae and distal ends of the maxillary and labial palps exhibit a strong signal, only low level of *nub* is present in the mandibles. (B) *nub* mRNA expression at 30% development. The signal resolves into several rings in the antennae and in thoracic legs. Expression is also observed in the posterior-most abdominal segment that corresponds to the presumptive proctodeum. (B′, inset) Close-up view of the head appendages at this stage shows the presence of three bands of *nub* in the antennae, a diffuse signal in the mandibles, and strong expression in the distal parts of the maxillary and labial palps. (C) At 50% development, new rings of *nub* appear in the antennae, maxillary and labial palps, and legs. Expression in the developing proctodeum remains. (C′, inset) At this stage, another band and a diffuse patch (asterisk) of *nub* emerge in the distal-most part of the antennae. In the maxillary and labial palps, two rings and a "sock" are observed in the proximal-mid region and at the distal-most end, respectively. (D–I) Magnified images of thoracic legs at 22%, 27%, 30%, 40%, 50%, and 60% development, respectively. (D) *nub* mRNA accumulates in the mid-distal region of each leg. (E) The expression pattern resolves into a series of rings, labeled I (proximal) and II (distal). (F–H) These rings expand in size (F) and eventually resolve into two additional rings. (G) First, the distal ring II splits into II_A and II_B, then the proximal ring I splits into I_A and I_B (H). The observed rings have varying levels of intensity with I_A, I_B, and the distal tip of the leg being the weakest. (I) As leg segments become apparent, there are several clusters of cells in the coxa and in the distal femur and tibia that continue to express *nub*. Scale bars: 100 μm. Abbreviations: An, antenna; Mn, mandible; Mx, maxilla; Lb, labium; T1–T3, thoracic legs 1–3; A1, first abdominal segment; Pr, proctodeum. Small Roman letters (a–b) denote *nub* expression in the maxillary and labial palps, whereas the Arabic (1–4) mark the rings of *nub* expression in the antennae. Roman numerals (I-II_B) represent expression domains of *nub* in the thoracic legs.

bars). The shortening of the T3 legs is slightly larger, totaling a 28.5% decrease in size. As shown in Fig. 2H (striped bars), the overall reduction in leg length is due to an uneven shortening of individual leg segments. The affected T2 leg femur, tibia, and tarsus exhibit 5.0%, 24%, and 56.2% reductions in size, respectively. A slightly larger effect is observed in the corresponding hind leg counterparts, ranging from 5.1% (femur) to 26% (tibia) to 63.9% (tarsus).

Acheta nub RNAi affects leg segmentation

Next, we focused on the T3 tibia and tarsus and examined the morphologies of their cuticular structures (spurs, spines, and bristles) (Figs. 3A–B2). In wild type hatchlings, the boundary between the first and second tarsomeres (Ta-1/Ta-2) bears two spines and a pair of spurs (Figs. 3A and A1). The spurs display a unique morphology by being covered with several bristles (Fig. 3A1, arrowheads). In contrast, the boundary between the tibia and first tarsal subunit (Ti/Ta-1) lacks spines and is surrounded by four spurs that are free of bristles (Fig. 3A2). A close examination of the corresponding structures in *nub*-depleted first nymphs reveals that morphology of the distal part of the tibia is greatly affected (Fig. 3B). First, the four bristle-free spurs that normally characterize distal tibia are absent. Second, this region now features the paired spurs (Fig. 3B1) and spines (Fig. 3B2) that are normally found at Ta-1/Ta-2 boundary. Furthermore, these spurs are covered with bristles similar to the ones observed at the distal end of the first tarsomere in wild type (compare Figs. 3A1 vs. B1, arrowheads). These findings show that in cricket *nub* RNAi first nymphs the tibia and Ta-1 fuse into a single segment displaying mixed characteristics, tibial at the proximal end and Ta-1 at the distal end.

nub and Ubx act in parallel to control the growth of Acheta hind legs

As illustrated in Fig. 2H, the tibia of *Acheta nub*-depleted individuals is 24% (T2) and 26% (T3) shorter compared to wild type. If one is to consider the fact that Ta-1 is actually incorporated into the tibia (i.e. *nub* RNAi Ti* = Ti + Ta-1), then the observed shortening is even more drastic. If we are to compare this podomere (Ti*) to wild type Ti + Ta-1, the actual reduction in its length would be about 52%. Thus, *nub* depletion not only causes the loss of the Ti/Ta-1 joint but also greatly affects the leg segment growth. Previous work in *Acheta* by Mahfooz et al. (2007) revealed that the Hox gene *Ultrabithorax* (*Ubx*) regulates the differential growth of T3 legs by causing their

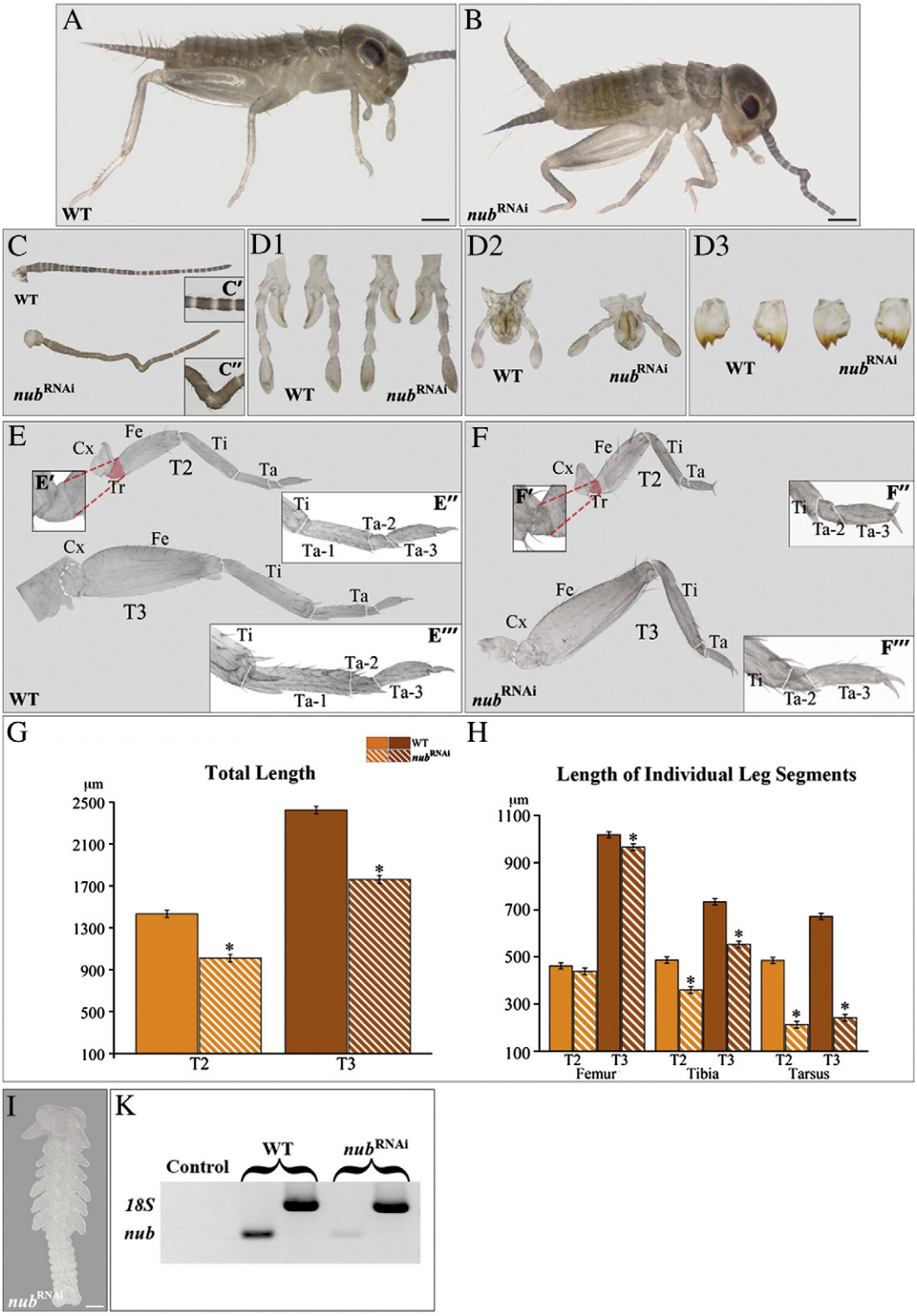

Fig. 2. *nub* RNAi phenotypes in *Acheta*. (A–B) Compared to wild type, class I hatchlings exhibit morphological changes in the head and thorax. (C–D3) Dissected antenna (C) and gnathal appendages: maxilla (D1), labium (D2), and mandible (D3) of wild type and *nub* RNAi first nymphs. The mid-distal region of the antenna becomes crooked in *nub*-depleted individuals (C′–C″), whereas the morphologies of their mouthparts remain unaltered. (E and F) Dissected T2 and T3 legs of wild type and *nub* RNAi hatchlings, respectively. (E′–E‴, F′–F‴, insets) The corresponding magnified images of the trochanter, distal tibia, and tarsus of wild type and *nub*-depleted individuals. Compared to wild type, *nub* RNAi legs have visibly reduced trochanter and no distinct first tarsomere. (G–H) Total leg length and the length of mid-distal segments in wild type and *nub*-depleted first nymphs, respectively. In the latter, the legs are significantly undersized due to the shortening of mainly the tibia and tarsus. (I) The accumulation of *nub* transcript is effectively abolished in *Acheta nub* RNAi embryos. (K) Compared to wild type, *nub*-depleted embryos show greatly reduced levels of *nub* mRNA. White solid lines mark the boundaries between the femur and tibia, tibia and tarsus, and each tarsomere, while broken lines separate the T3 coxa from the body wall. Error bars represent the 95% confidence intervals, n = 16. $^{*}p<0.05$ as determined by ANOVA. Scale bars: 200 µm (A and B); 100 µm (I). Abbreviations: WT, wild type; T2–T3, thoracic legs 2–3; Cx, coxa; Tr, trochanter; Fe, femur; Ti, tibia; Ta, tarsus; Ta 1–3, tarsomeres 1–3.

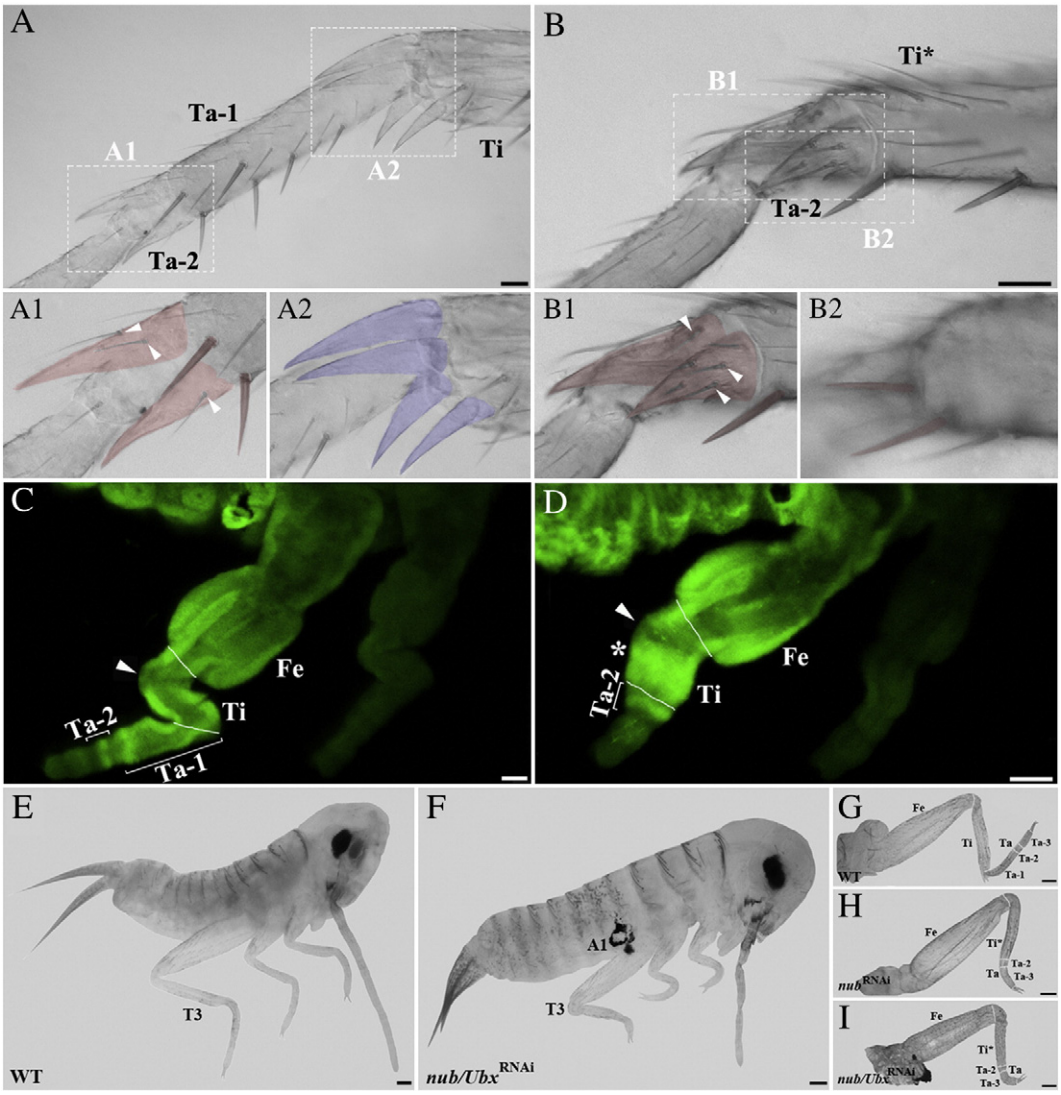

Fig. 3. *nub* and *Ubx* are required for proper leg formation in *Acheta.* (A–B) Magnified images of the metathoracic tibia and tarsus of wild type and class I first nymphs, respectively. (A1–A2) Close-up views of the boundaries between the first and second tarsomeres (A1) and between the tibia and first tarsomere (A2) in wild type. In order to better visualize their morphologies, spines and spurs were artificially colored. Ta-1/Ta-2 boundary bears a pair of spines and two spurs covered with bristles (arrowheads), while four spurs free of bristles surround Ti/Ta-1 boundary. (B1–B2) Close-up views of the corresponding structures in *nub*-depleted individuals. The distal region of the tibia now bears one pair of spurs covered with bristles (B1, arrowheads) and one pair of spines (B2), both cuticular features that are normally found on the first tarsomere. (C, D) *Ubx* expression patterns in the hind legs of wild type and *nub*-depleted embryos, respectively. (C) The T3 legs of wild type *Acheta* embryos exhibit an ectodermal *Ubx* expression in the tibia and mesodermal signal in the femur, first and second tarsomeres. (D) In contrast, *nub* RNAi embryos have a novel mesodermal expression of *Ubx* in the mid-distal region of the tibia (asterisk) and a single ring in the tarsus that corresponds to the second tarsomere. In both panels, an arrowhead indicates the absence of signal in the small area of the proximal tibia. (E, F) Lateral views of wild type and *nub*/*Ubx* RNAi embryos, respectively. The latter grows ectopic appendages on the first abdominal segment and has severely shortened thoracic legs. (G–I) Dissected hind legs of wild type (G), *nub* RNAi (H), and *nub*/*Ubx* RNAi embryos (I). Compared to wild type and *nub* RNAi alone, the T3 legs of double *nub*/*Ubx* RNAi embryos are more drastically reduced in size due to a significant shortening of the femur, tibia, and tarsus. White solid lines mark the boundaries between individual segments. Scale bars: 50 μm (A, B, C, and D); 100 μm (E–I). Abbreviations: WT, wild type; T3, hind leg; Fe, femur; Ti, tibia; Ta, tarsus; Ta 1–3, tarsomeres 1–3; Ti*, fused tibia and first tarsomere; A1, first abdominal segment.

mid-distal segments (femur, tibia, and tarsus) to differentially enlarge compared to the corresponding T2 leg counterparts. Hence, by focusing on T3 legs (where both *nub* and *Ubx* are expressed) we can examine the relationship between these two genes with regard to leg growth.

In wild type, *Ubx* accumulates in both the ectoderm and mesoderm of the femur and along a rim of ectodermal cells in the tibia (Fig. 3C). Note that a patch of cells in the proximal region of the tibia is devoid of *Ubx* expression (Fig. 3C, arrowhead). In the first tarsomere (Ta-1), *Ubx* expression is localized not only in the ectoderm but also in a ring of the mesodermal cells at its distal end. Another mesodermal ring of *Ubx* expression is seen in the presumptive Ta-2, while there is no detectable expression in the third tarsal subunit. These findings show that accumulation of *Ubx* in the tibia is solely ectodermal, whereas its localization in the femur and first tarsomere is both ectodermal and mesodermal.

As depicted in Fig. 3D, in similarly staged *nub*-depleted embryos, *Ubx* expression remains unchanged in the femur and proximal half of the tibia. Note that the small region devoid of *Ubx* signal (Fig. 3D, arrowhead) is still present in the tibia. However, the distal tibia now acquires a strong ectopic mesodermal expression of *Ubx* (Fig. 3D, asterisk). In addition, the tarsal *Ubx* accumulation becomes restricted to a single band of the cells corresponding to the second tarsomere of wild type. This observed pattern of *Ubx* in the tibia and tarsus is consistent with the physical changes in the morphology of these two segments in *nub*-RNAi embryos (the severe tissue compression and fusion of the distal tibia and proximal-most tarsus). We interpret the novel expression of *Ubx* in the mesoderm of the tibia (Fig. 3D,

asterisk) as being caused by tissue re-arrangement rather than an indication of putative regulation by *nub*, since no evidence of such control is observed in any other T3 leg segment.

To explore the above interpretation further, we examined the possible interactive effects of *nub* and *Ubx* on the elongation of *Acheta* T3 legs by simultaneously depleting these genes using RNAi (Figs. 3F and I). The double RNAi embryos do not hatch, although they do complete about 85% of embryogenesis (Fig. 3F). These individuals display a phenotype that combines the previously observed effects of each gene separately. In the A1 segment, there is a formation of an ectopic leg-like appendage due to the failure of *Ubx* to repress *Distal-less*, *Dll* (Mahfooz et al., 2007). Furthermore, double *nub*/*Ubx* RNAi embryos are characterized by T3 femur, tibia, and tarsus that are smaller than those found in either single *Ubx* (Mahfooz et al., 2007) or *nub* RNAi applications (Figs. 3H and I). These results appear to indicate that each gene acts in an additive fashion, further supporting the notion that *nub* and *Ubx* regulate T3 leg growth independently.

Drosophila nub controls joint formation and development of claws

The leg phenotype observed in *Acheta nub* RNAi first nymphs, however, was not reported in either *Oncopeltus* or *Drosophila* where *nub* functions were also studied. Because hypomorphic *nub* mutant flies were described as exhibiting "shortened and gnarled" legs (Cifuentes and Garcia-Bellido, 1997), we decided to characterize this phenotype in more detail by generating *nub* null individuals nub^{E37}/*Df nub*- (see Materials and methods). nub^{E37} is a null allele that produces no protein (Yeo et al., 1995) and shows no overt mutant phenotype during embryogenesis (Hrycaj et al., 2008; Yeo et al., 1995), whereas the *nub*- deficiencies employed (see Materials and methods) completely remove the *nub* gene and its adjacent tandem paralogue *pdm*-2 (Yeo et al., 1995). However, a few nub^{E37}/*Df nub*-escapers were able to reach the pupal stages but they died as pharate adults inside the pupal cases that could be dissected to show their leg phenotype.

The expression of *nub* in *Drosophila* was previously described as being localized near the developing leg joints at late third instar (Rauskolb and Irvine, 1999) and late pupal stages (Mirth and Akam, 2002). In this study, we analyzed the expression patterns of both *nub* and *odd-lacZ* reporter in the legs of wild type pupae between 4 and 12 h after puparium formation (APF) (Figs. 4A and B) and that of *odd-lacZ* in the adult prothoracic legs of wild type males (Fig. 4C). Between 4 and 12h APF, the expression of *nub* is proximally adjacent to that of *odd-lacZ* (Fig. 4A), which in turn, labels the proximal part of all joints except those between tarsal subsegments (Fig. 4C; (Mirth and Akam, 2002)). This expression pattern tightly correlates with the leg defects observed in nub^{E37}/*Df(2L)GR4* individuals, which are characterized by the absence of the joints between the coxa, trochanter, femur, and tibia (Fig. 4D). These mutants also exhibit the loss of tissue proximal to these joints that leads to the appearance of fused leg segments, and in some cases, to the elimination of the entire tarsal subunit. The most visible changes are observed in the tibia and tarsus. The former acquires the sex combs (sx) that are normally found at the distal end of the first tarsomere (Ta-1), which correlates with the fusion of Ti and Ta-1 (Fig. 4D, inset). The tarsus also loses the fifth tarsomere (Ta-5) that, in turn, entails the loss of the attached claw (Fig. 4D). In addition, these mutants have the femur fused to the proximal end of the tibia (Fig. 4D, arrow). We also observed a slightly milder phenotype in two individuals out of 15 studied, where the claw and Ta-5 remain, albeit the latter is reduced and fused to the fourth tarsomere (Fig. 4E). Note that these flies still have fused tibia–tarsus (Ti*), and thus strikingly resemble the legs of *Acheta* first nymphs treated with *nub* dsRNA. Finally, we generated flies mutant for *pdm*-2 (Yeo et al., 1995), which displayed wild-type looking legs (not shown) corroborating that the *nub* phenotype described above represents solely the true null condition for *nub* in legs.

Periplaneta nub has a role in the proper development of antenna and in leg segmentation

The expression of *nub* in *Periplaneta* was described previously (Li and Popadić, 2004), revealing distinct patterns in head appendages and legs. Here, we extended the original study to include earlier embryonic stages of *nub* expression in legs as well as RNAi analysis. At 15% development, *Periplaneta nub* is expressed in the mid-distal limb buds (Fig. 4F). By 18% development, *nub* expression is in two broad rings at the proximal and medial limb positions (Fig. 4G). As embryogenesis proceeds, these two rings first split, as observed in *Acheta*, and then a new ring is added to eventually result into five rings (Fig. 4H). At 30% development, *nub* expression coincides with the establishment of distinct leg segments (Fig. 4I). We analyzed the function of *nub* in *Periplaneta* via RNAi and examined a total of 567 individuals, of which 266 were wild type and 301 exhibited *nub* RNAi phenotypes. Overall, the effect in *Periplaneta* is very similar to the one observed in *Acheta*, characterized by changes in antennae and legs and no visible changes in mouthparts (Fig. 5). Furthermore, as reported for other insects where its function has been examined so far (Bhat and Schedl, 1994; Hrycaj et al., 2008), the majority of *nub* RNAi cockroaches are embryonic lethals (n = 228), completing about 95% of development. Occasionally, some embryos manage to hatch into first nymphs but die soon after (n = 73).

Depending on the severity of the observed changes, *Periplaneta nub*-depleted individuals can be divided into two classes, moderate and strong. In moderate phenotypes, the antenna is the only head appendage that is affected (Fig. 5B). Compared to wild type, it is shorter with its distal-most part being bent and lacking segmentation (Figs. 5B′ and B″). In strong phenotypes (Fig. 5E), this appendage undergoes further size reduction and becomes unsegmented along its entire length (Figs. 5F–F″). The other major *nub* RNAi effect is observed in legs. The wild type legs of running (cursorial) insects, such as cockroaches, are characterized by having a broad coxa, a minute triangular shaped trochanter, and elongated femur, tibia, and tarsus (Fig. 5C). In addition to being wide, the coxa has the distinct suture (white arrow) and a "bulge" (black arrow) at its distal end (Fig. 5C″). In moderately affected *Periplaneta nub* RNAi hatchlings, the trochanter is reduced in size (compare Figs. 5C″ vs. D′) similar to phenotypes observed in *Acheta*. In more seriously affected animals, the trochanter is completely lost as an independent segment and becomes fused to a shortened coxa (Fig. 5D‴, black arrowheads). This creates a combined Cx/Tr-Fe joint with mixed characteristics (Fig. 5D″). This is similar to the situation observed in *Drosophila* nub^{E37}/*Df(2L)GR4* individuals, which display lack of joints and partial fusions between Cx, Tr, and Fe (Fig. 4D). In strong *Periplaneta nub* RNAi phenotypes, we observe an additional leg defect (Fig. 5G). Besides having a fused coxa–trochanter (Fig. 5G′), these embryos also have malformed T2 and T3 tibia (Figs. 5G and G″). A closer examination reveals that this segment actually curves back on itself forming a ball of tissue, while still retaining a pair of tibia-specific spurs on its distal end (orange arrowheads in Figs. 5C and G″). Furthermore, the joint between the femur and tibia (Fig. 5G″, black arrowheads) is lost. Note that the lack of the same joint occurs in *nub* mutant flies (Fig. 4D, arrow).

Acheta and Periplaneta nub have no role in the abdomen formation

Hrycaj et al. (2008) showed that in *Oncopeltus*, the depletion of *nub* causes the growth of ectopic legs on segments A2 to A6. While *nub* signal is also detected in both *Acheta* and *Periplaneta* abdomens, its expression is restricted to the developing proctodeum (Li and Popadić, 2004). Despite this presence of *nub* expression, no morphological changes were observed in this structure following RNAi treatment. Hence, these data indicate that *nub* has no overt function in the development of *Acheta* and *Periplaneta* abdomens.

Discussion

Although the expression of *nub* has been analyzed in several insects, its functional significance has been explored only in the dipteran *Drosophila* and the hemipteran *Oncopeltus*. Here, we examine the roles of *nub* in an orthopteran, *A. domesticus* and a dictyopteran, *P. americana*. Both species exhibit an ancestral mandibulate-type of mouthparts and belong to phylogenetically more basal lineages compared to milkweed bugs. In addition, we characterize in more detail the leg phenotype of *Drosophila nub* mutants. We found that while *nub* plays a role in the growth of specific leg segments in all four species, its requirement in joint formation might be only shared between *Drosophila*, *Acheta*, and *Periplaneta.* Interestingly, *nub*-depleted embryos of the latter three species do not exhibit ectopic abdominal appendages, a phenotype that is observed in *Oncopeltus*. These findings suggest the presence of species-specific variations in the genetic mechanisms underlying leg segmentation and growth as well as the formation of a limbless abdomen in insects.

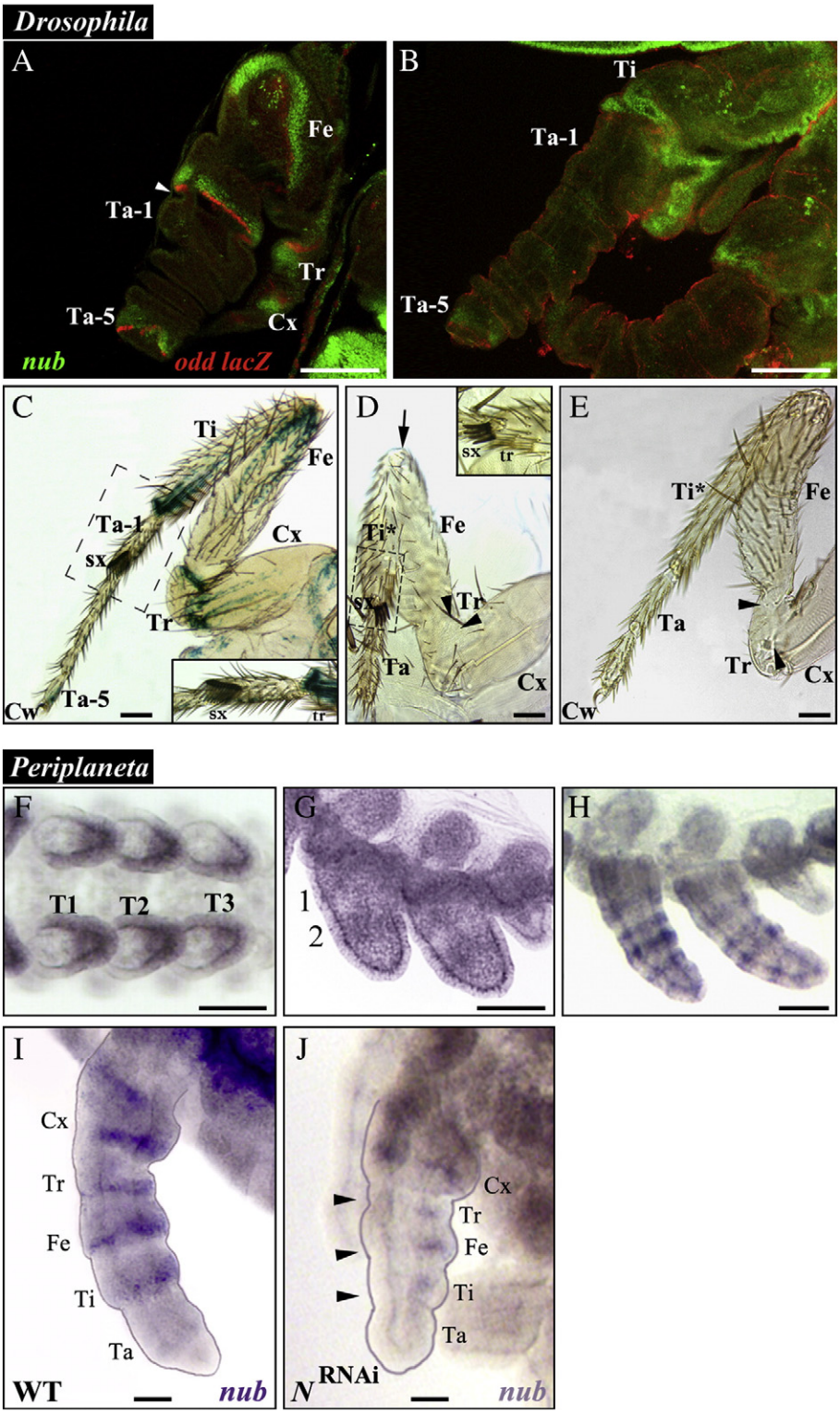

Role of nub in the head

Based on the expression and functional data reported in *Oncopeltus*, it was suggested that *nub* might play an important role in the morphological diversification of insect mouthparts (Hrycaj et al., 2008; Li and Popadić, 2004). Milkweed bugs have a haustellate-type mouth where the mandibular and maxillary appendages are structurally similar but anatomically different from the labium. In this species, *nub* is expressed in all head appendages and its depletion affects the size of the labium and the formation of antennal sensilla. The role of *nub* in the development of mandibular (Mn) and maxillary (Mx) appendages, however, could not be inferred because *nub* RNAi individuals do not complete embryogenesis and these structures are extruded only upon hatching.

In contrast to the situation in *Oncopeltus*, gnathal appendages in *Acheta* and *Periplaneta* are already formed by the end of embryogenesis and are easily distinguished from each other in both late embryos and in first nymphs. Both species have mandibulate mouthparts where the maxillary and labial (Lb) appendages share a similar anatomy that is distinct from the mandibles (Hrycaj et al., 2010; Popadić et al., 1998). These appendages also display a nearly identical patterning of *nub* expression. However, despite this observation, we do not detect any morphological changes in the Mx and Lb appendages of *Acheta* (Figs. 2D1 and D2) and *Periplaneta nub* RNAi hatchlings (not shown). These individuals also show no effect in the mandibles (Fig. 2D3). In fact, the only head appendage that exhibits a phenotype is the antenna that becomes bent in both species. In *Acheta*, the effect is localized to its mid-distal portion, which corresponds to two rings (bands 3 and 4) of *nub* expression (Figs. 2C and 1C′, inset). A much stronger phenotype is observed in *Periplaneta*, where the antenna is visibly reduced in size and lacks segmentation (Figs. 5F–F″). Overall, our data highlight the varying degree of *nub* function in antennal development, ranging from affecting only sensilla formation (*Oncopeltus*) to regulating its elongation and segmentation (*Periplaneta*). Furthermore, despite its expression in all of the gnathal segments, *nub* was shown to affect only labial appendages in one species (*Oncopeltus*) and to have no effect in *Periplaneta* and *Acheta*.

Role of nub in the legs

As illustrated in Fig. 6, diverse patterns of *nub* expression are observed in the developing legs of different insect species. In a basal, primitively wingless insect *Thermobia*, *nub* is localized in three clusters of cells in the proximal leg region (Li and Popadić, 2004). In *Periplaneta, nub* pattern is composed of five rings each corresponding to a presumptive segment. With some modifications, this pattern is also observed in holometabolous fruit flies (*Drosophila)* and in another hemimetabolous species, *Acheta*. Among the rings, those corresponding to the femur and tibia are thinner in *Periplaneta* and *Drosophila* compared to *Acheta*. In *Oncopeltus*, the trochanter ring is absent and the legs gain a letter H-like pattern in the presumptive tibia and tarsus. Overall, these observed patterns suggest that in winged insects, *nub* has a role in segment growth and/or joint formation. It would appear though, that this role is not completely conserved, and that depending on the lineage, it may encompass all leg segments (flies and cockroaches) or just some (milkweed bugs and crickets).

As shown in Fig. 4D, *Drosophila* $nub^{E37}/Df(2L)GR4$ mutants lack claws, the fifth tarsomere, and the joints between the tibia, femur, trochanter, and coxa. A closer inspection also reveals that the tibia and the first tarsomere (Ta-1) fuse to form a single segment. This phenotype, with the tibia featuring Ta-1 characteristics in its distal region (Fig. 4D, inset), is identical to the morphology of the fused tibia/Ta-1 observed in *Acheta nub* RNAi legs (Figs. 3B–B2). Hence, in these two insects, *nub* seems to be involved in the development of the distal part of segments and of the adjacent joints. This role is also present in *P. americana*, a dictyopteran (the sister clade of the Orthoptera, grasshoppers and crickets), where *nub* RNAi phenotypes are characterized by fused coxa and trochanter along with concomitant loss of joints between these two segments. In *Oncopeltus*, however, the depletion of *nub* affects the size and shape of the femur but has no effect on leg segmentation (Hrycaj et al., 2008). These results indicate that while the function of *nub* in leg segmentation has been maintained in *Periplaneta*, *Acheta,* and *Drosophila*, it has been modified in *Oncopeltus*. At the same time, all of these species exhibit varying levels of segment shortening in the absence of *nub,* which suggests that its role in leg growth has been conserved in all of them, albeit to a different degree. Because our data were generated by using the RNAi to investigate a gene function, it is possible that resulting phenotypes might not correspond to true nulls but to a range of hypomorphic mutants. In other words, *nub* function may still be required in all segments where *nub* is expressed and not only in those showing an overt morphological change. However, the observed differences in its expression patterns (Fig. 6), especially at earlier stages, suggest that *nub* roles in leg development may indeed be species-specific. For example, the strong early embryonic signal (dark blue rings in Fig. 6) can be associated with the distinct leg phenotypes in *Periplaneta* or *Acheta*. Note that because these strong expression patterns precede the stage at which leg becomes fully segmented, their depletion is likely to affect the growth and development of some, but not all, of the segments.

In *Drosophila*, the expression of *nub* is present in specific positions along the developing leg where stripes of Notch signaling appear (Bishop et al., 1999; de Celis et al., 1998; Rauskolb and Irvine, 1999). Notch signaling controls the expression of several genes to position the joints and to specify different proximal and distal subdomains within the joint (Bishop et al., 1999; Mirth and Akam, 2002; Rauskolb and Irvine, 1999). In particular, the expression of *nub* was shown to depend on Notch signaling (Greenberg and Hatini, 2009; Rauskolb and Irvine, 1999). Thus, we can envisage *nub* as being involved in a

Fig. 4. *nub* expression and mutant phenotypes in *Drosophila* and expression patterns of *Periplaneta nub* mRNA in wild type and *Notch* RNAi embryos. (A) Developing *Drosophila* leg at 4–8 h after puparium formation (APF) when eversion of the leg from the leg disc is underway, stained for *nub* (green) and *odd-skipped lacZ* (*odd-lacZ*, red) expressions. *nub* expression is adjacent and proximal to that of *odd-lacZ*. *odd-lacZ* expression labels the proximal side of the joints between the pretarsus and fifth tarsomere, between the first tarsomere and tibia, between the tibia and femur, between the femur and trochanter, and between the trochanter and coxa. At this stage, the joints appear as constrictions in the tissue (white arrowhead). (B) Developing *Drosophila* leg at 8–12 h APF, showing *nub* (green) and *odd-lacZ* (red) expressions. The leg segments are fully everted and continue to elongate to their final sizes, while the leg joints still appear as constrictions between segments. (C) Adult prothoratic male leg stained for *odd-lacZ* expression. Notice the expression of *odd-lacZ* at the proximal side of Ti/Ta-1 joint and at the fifth tarsomere just proximal to the claw. (C, inset) Close-up view of the Ti/Ta-1 boundary showing the presence of the transverse rows of bristles (tr) and sex combs (sx) at the distal ends of the tibia and first tarsomere, respectively. (D) Adult prothoratic leg from a $nub^{E37}/Df(2L)GR4$ male. All structures exhibiting *nub* expression in A and B are defective: Ta-5 and the claws are lost, the tibia and first tarsomere are fused together, and the joints between the tibia and femur (arrow), the femur and trochanter (black arrowhead), and the trochanter and coxa (black arrowhead) have not formed. (D, inset) Close-up view of the Ta/Ta-1 boundary showing sex combs and transverse row of bristles joined together due to the loss of the tissue in between. (E) Rare mild phenotype displayed by a $nub^{E37}/Df(2L)prd1.7$ leg. While Ta-5 has not formed properly, the claws are still present at the tip of the leg. In addition, the first tarsomere is fused to the tibia and the joints between the tibia and femur, the femur and trochanter (black arrowhead), and the trochanter and coxa (black arrowhead) have not formed completely. (F–I) *nub* expression in developing legs of *Periplaneta*. (F) In the early limb bud stage, *nub* is expressed from the middle to distal tip of each leg. (G) As the legs develop further, two broad rings of *nub* expression appear in their proximal (1) and medial (2) portions. (H) These rings eventually split and a new ring appears at the distal tip of the leg, giving a total of five rings. (I) As leg segments become visible, *nub* expression is localized proximal to each joint, with the exception of the tarsomeres (not shown). (J) While *nub* signal is reduced in *N*-RNAi treated embryos of comparable age, it can still be observed in Tr, Fe, and Ti (black arrowheads). Scale bars: 50μm. Abbreviations: WT, wild type; Cx, coxa; Tr, trochanter; Fe, femur; Ti, tibia; Ti*, fused tibia and first tarsomere; Ta, tarsus; Ta 1–5, tarsomeres 1–5; Cw, claws; sx, sex combs; tr, transverse row of bristles. T1–T3, thoracic legs 1–3.

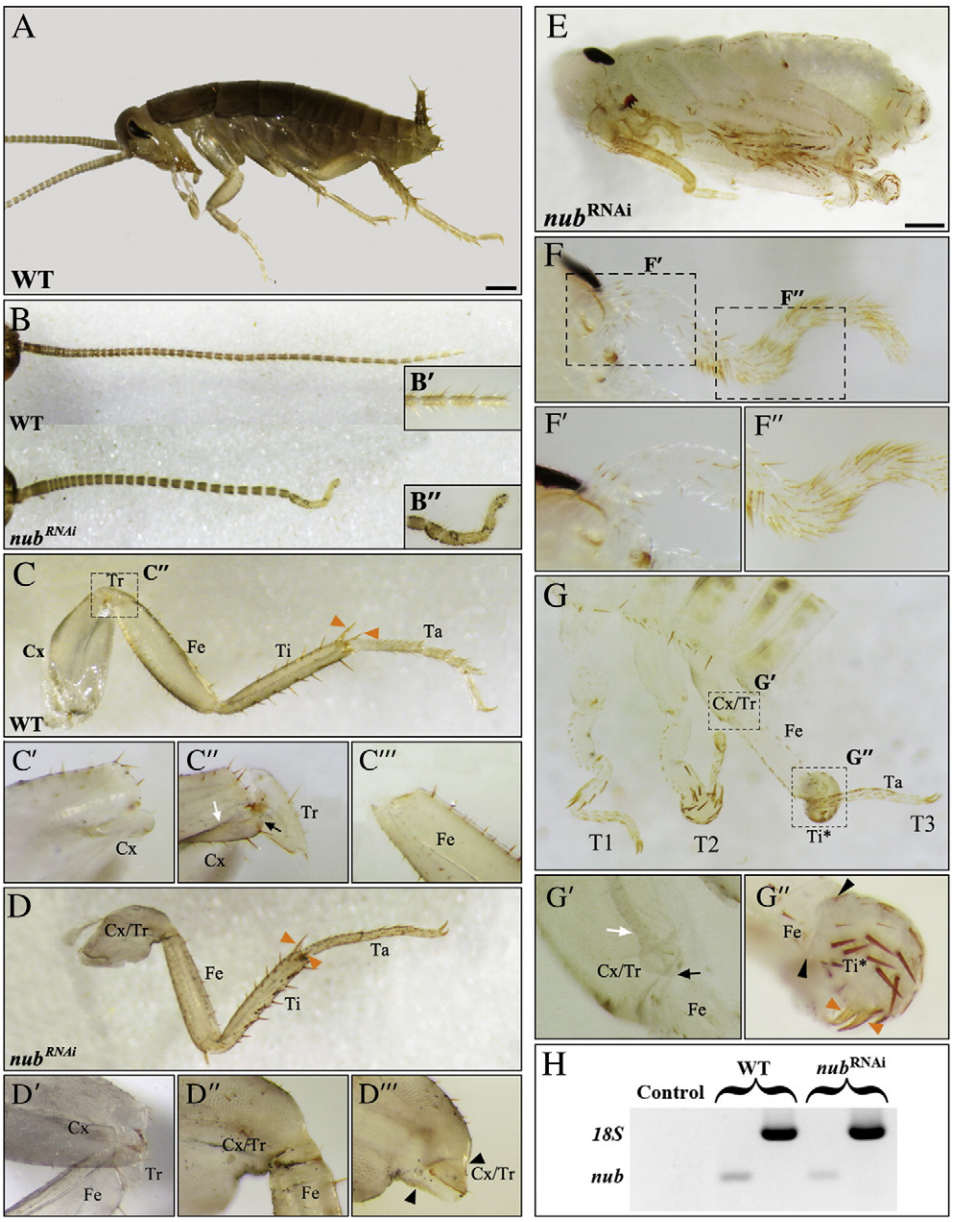

Fig. 5. *nub* RNAi phenotypes in *Periplaneta americana*. (A) Lateral view of wild type first nymph. (B) Dissected antennae of wild type (top) and moderately affected *nub*-depleted individuals (bottom). The latter is visibly shortened and abnormally bent at its distal-most end. (B′–B″, insets) Close-up views of the corresponding antennal regions showing loss of segmentation in *nub* RNAi first nymphs (B″) compared to wild type (B′). (C) Dissected T3 leg of wild type. (C′–C‴) Close-up views of the distal coxa (C′), the boundary between the coxa and trochanter (C″), and of the proximal femur (C‴). The distal coxa is characterized by the presence of suture (white arrow) and a "bulge" (black arrow). (D) Dissected T3 leg of moderately affected *nub*-depleted individual. (D′–D‴) Close-up views of the greatly reduced Tr (D′), Cx/Tr-Fe joint (D″), and fused coxa–trochanter (D‴). Compared to wild type (C″), the coxa and trochanter become fused together as a result of the joint loss between these two segments (black arrowheads). (E) Lateral view of strongly affected *nub* RNAi embryo. (F) Dissected antenna of *nub* RNAi individual showing severe reduction in size and bending along its entire length. (F′–F″) Close-up views of its proximal and mid-distal regions showing loss of segmentation. (G) T1, T2, and T3 legs of strong phenotype. (G′–G″) Strongly affected *nub* RNAi individuals do not only lose a joint between Cx and Tr (G′) but also between Fe and Ti (black arrowheads in G″). The black arrow points to the "bulge" of coxa, which marks the distal-most portion of this segment. Note that while the T3 tibia is deformed, it still retains a pair of spurs (orange arrowheads) at its distal end that are also found in a moderate *nub* RNAi phenotype (panel D) and in wild type (panel C). (H) RT-PCR analysis of *nub* mRNA in late embryos showing only trace levels in *nub*-depleted individuals compared to wild type. Scale bars: 500 μm. Abbreviations: WT, wild type; T3, hind leg; Cx, coxa; Tr, trochanter; Fe, femur; Ti, tibia; T*, deformed tibia; Ta, tarsus; Cx/Tr, fused coxa and trochanter.

Notch-dependent leg patterning process that leads to the growth of the distal parts of the leg segments and the development of the adjacent joints (Fig. 7). Insights from studies in *Drosophila* and *Cupiennius* support this notion, showing that Notch-dependent formation of joints is linked to the proper growth of the leg segments (Bishop et al., 1999; de Celis et al., 1998; Prpic and Damen, 2009; Rauskolb and Irvine, 1999). This scenario is consistent with both the hypothesis that Notch signaling during joint development is conserved among arthropods (Prpic and Damen, 2009) and our findings that the levels of *nub* expression are reduced following *Notch* RNAi in *Periplaneta* (Figs. 4I and J).

As illustrated in Fig. 6, *nub* patterns are equally diverse in crustaceans encompassing two (*Porcellio scaber*, a woodlouse) to four rings of expression (*Pacifastacus leniusculus*, a crayfish), and in a spider, *Cupiennius salei* (Abzhanov and Kaufman, 2000; Damen et al., 2002; Prpic and Damen, 2009). However, in another spider species, *Steatoda triangulosa*, only a single segmental ring of expression exists in the legs (Abzhanov and Kaufman, 2000). These data show that

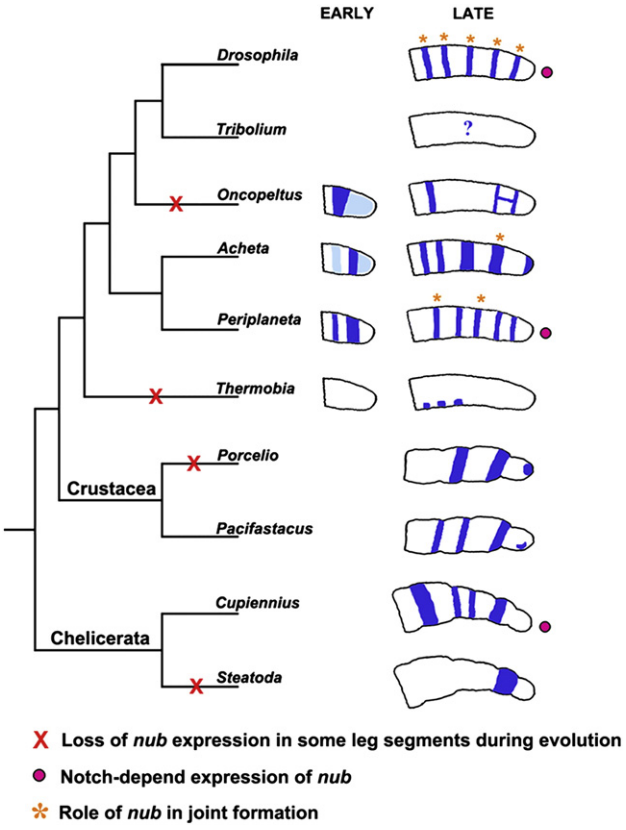

Fig. 6. Summary of changes in *nub* expression and function during arthropod evolution. In the primitively wingless insect *Thermobia*, the expression of *nub* is confined to three patches of cells in the proximal half of the leg. In winged insects, starting with *Periplaneta*, multiple rings of expression are observed that correspond to individual leg segments. In *Oncopeltus*, several rings are absent and the two distal-most rings are linked forming a letter H-like pattern. Functional analysis from this work and other (see text) indicates that *nub* is important for leg segment growth and joint formation in winged insects. The requirements for the latter function (orange stars) differ among species studied and may encompass all leg joints, such as in *Drosophila*, or just few (*Acheta* and *Periplaneta*). The role of *nub* has not been studied outside of the insects, but its expression patterns have been examined in other arthropod species, including crustaceans and chelicerates. In both groups, *nub* is expressed in all or most leg segments, with the exception of *Steatoda*. These data indicate repeated instances of loss (red X) and/or acquisition of *nub* expression during arthropod evolution. Several lines of work in *Drosophila, Periplaneta*, and *Cupiennius* (see text for details) show that *nub* expression in these organisms is dependent on Notch signaling (pink circles).

during arthropod evolution, there were repeated instances of either loss or acquisition of *nub* expression in leg segments, depending on the lineage. As illustrated by our results in Figs. 3–5, these changes of expression may have led to the eventual changes in the morphology of leg segments in insects.

The question that arises is how was this variability in the pattern of expression of *nub* achieved during evolution? Accepting that Notch signaling is deployed in all joints across arthropods, changes in the sensitivity of *nub* to Notch-mediated activation do not offer a simple way to explain the observed variation in *nub* expression. However, several pieces of evidence suggest that a local, Notch-independent factor is also involved in *nub* activation (Fig. 7). First, the elimination of the Notch ligand *Delta* (*Dl*) in *Drosophila* does not produce a total loss of *nub* expression (Campbell, 2005). Second, there are contradictory reports as to whether ectopic expression of *Dl* can induce ectopic expression of *nub* (Campbell, 2005; Rauskolb and Irvine, 1999). The most parsimonious explanation for reconciling these reports would be to propose that *Dl* requires a non-ubiquitous co-factor to activate *nub*. As a consequence, only in those experiments where ectopic *Dl* expression coincides with this factor, an ectopic activation of *nub* would be achieved. Third, *N*-RNAi in both *Periplaneta* (Fig. 4J) and spider *Cupiennus* (Prpic and Damen, 2009) causes only a moderate loss of *nub* expression in the legs. In the former case we can also document that the administration of *N* dsRNA eliminates most of *N* transcript (Pueyo et al., 2008). Hence, at least in *Periplaneta*, the requirement of *N* for *nub* expression cannot be very stringent. Fourth, the expression of *nub* in *Drosophila* has been shown to coincide with *Bar* and to be regulated by *C15* and *Al* (Campbell, 2005). These are proximal–distal patterning genes (Couso and Bishop, 1998) that are segment-specific and act independently or upstream of Notch (Rauskolb, 2001). In our diagram (Fig. 7), we refer to this local, Notch-independent factor as an X, but it follows from the previous discussion that this local factor may in fact be a collection of factors, each specific for a given leg segment(s). The evolution of *nub* expression, in particular the gains or losses of *nub* in specific leg segments, may simply reflect either changes in proximal–distal gene expression or changes in the sensitivity of the *nub* gene to the input of these genes. Given that proximal–distal leg patterning is remarkably conserved across the arthropods (Abzhanov and Kaufman, 2000; Panganiban et al., 1995; Prpic et al., 2003, 2001; Pueyo and Couso, 2005), the simplest hypothesis is that the observed variability in *nub* leg expression is due to changes across species in the *nub* gene enhancers that respond to X gene(s), most of which encode putative transcription factors. Alternatively, the variability in *nub* expression could be due to species-specific changes in the expression of these segment-specific X genes. This scenario could also offer an explanation for the variability of *nub* phenotypes that are observed in different species (as illustrated in Fig. 7). The Nub protein must interact with other genes and proteins to carry out its functions, and it is possible that such Nub interactors are deployed differently in different segments in different species. These alternative hypotheses (changes in *nub* gene cis-enhancers vs. changes in the expression of *nub* trans-interactors) provide simple, and eventually testable, mechanisms to explain the evolution of *nub* expression and function in arthropod legs.

In terms of their body plan, while the division of insect legs into five segments is a conserved feature, the morphology of each leg segment is not. As a matter of fact, it is the differences in the leg segment size, shape, and pigmentation that account for a significant amount of species-specific differences. For example, all cockroaches (Blattodea) share the enlarged coxa on all three pairs of legs that distinguish them from other insects at the order level. What differentiates various cockroach species, however, are the traits such as variation in number of the femoral spines on T1 legs or the number and size of attachment pads on the tarsal subsegments. In contrast, crickets (Orthoptera) always have a small coxa on all legs and it is the enlarged femur and tibia of hind legs that distinguish this insect group. With regard to individual cricket species, they can be differentiated by variation in the number of their tarsomeres or by the presence of armature on their T3 tibia. While all of these traits are genetically controlled, whether a controlling gene behaves as "variable" or "conserved" will depend on the degree of morphological change, which in turn, will depend on the taxonomic level under study. What we have learned so far is that the general framework of leg patterning is highly conserved in insects and regulated by *hth*, *dac*, and *Dll* (Angelini and Kaufman, 2004; Casares and Mann, 2001; Mardon et al., 1994; Ronco et al., 2008; Suzuki et al., 2009; Wu and Cohen, 1999). These three genes establish the proximal, mid, and distal leg regions, and their expression patterns are shared between species as different as *Drosophila*, *Tribolium*, *Gryllus*, and *Oncopeltus* (Abu-Shaar and Mann, 1998; Angelini and Kaufman, 2004; Beermann et al., 2001; Inoue et al., 2002; Prpic et al., 2001; Ronco et al., 2008; Wu and Cohen, 1999). The present study of *nub* illustrates how genes with variable expression may be in fact more important from an evolutionary point of view, than those whose expression remains constant. Hence, our focus should shift to identifying other "variable" genes, perhaps ones that act downstream of the proximal–distal

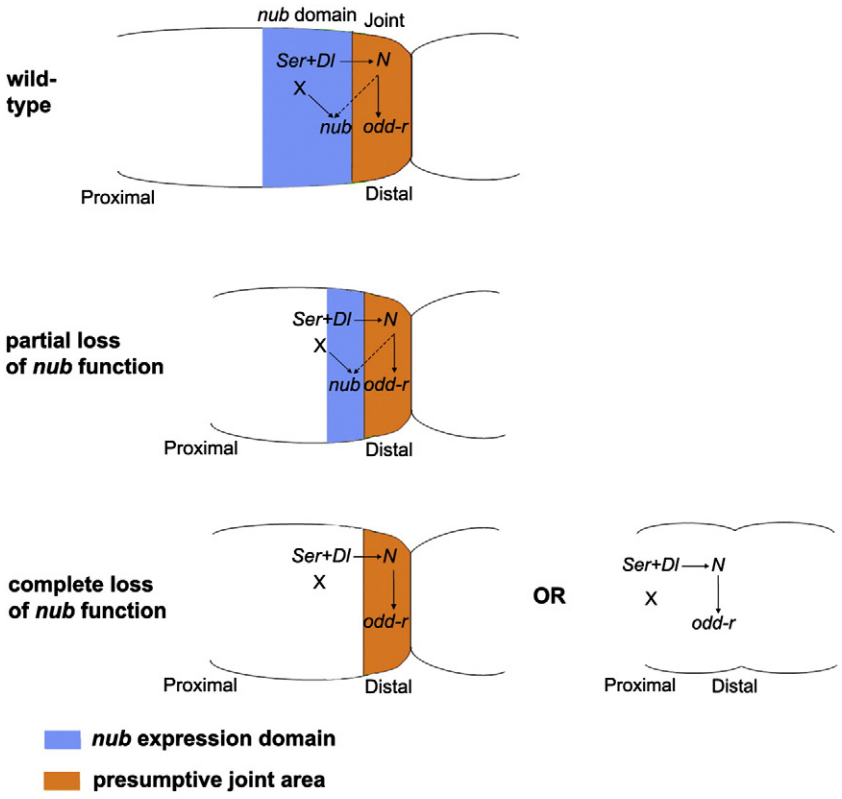

Fig. 7. Model for the regulation and function of *nub* in insect legs. Solid arrows denote direct gene and protein interactions, while broken arrows represent indirect ones. The expression of *nub* (blue) is activated proximal to the presumptive joint area (orange). Notch signaling sets up both of these territories. Cells expressing the Notch ligands *Serrate (Ser)* and *Delta (Dl)* appear between presumptive leg segments. These *Ser* and *Dl* expressing cells do not signal to each other but to the adjacent distal cells that will form the presumptive joint itself. The activation of the Notch signaling pathway in these distal cells leads to the activation of direct Notch targets, such as the *odd-r, E(spl),* and *bib* genes (Bishop et al., 1999; de Celis et al., 1998; Rauskolb and Irvine, 1999). Note that although Notch signaling is required for *nub* expression, *nub* is not activated in the presumptive joint cells, but proximal to them, essentially coinciding with *Ser* and *Dl* expression (Fig. 4C) (Campbell, 2005; Greenberg and Hatini, 2009; Mirth and Akam, 2002). Hence, the expression of *nub* must be indirectly activated by a secondary, Notch-dependent signal (broken arrow). In addition to this Notch-dependent signal, the evidence suggests that *nub* expression may require another input from a Notch-independent local factor (X) (see text). The function of *nub* is to promote the growth and development of the cells proximal to the joint, which in turn, are required for a correct morphogenesis and differentiation of the joint. In legs suffering a partial lack of *nub* function, the territory proximal to the joint (orange) is reduced; the leg segment appears smaller but the joint still forms. In legs with a total loss of *nub* (or beyond a certain threshold), the whole *nub*-expressing territory is lost resulting in two alternate outcomes. First, the segment may be reduced, although the joint remains unaffected (e.g. the femoral segment in *Oncopeltus* or the trochanter in *Acheta*). Second, the segment shortens and the joint fails to form. This, in turn, causes segments to fuse (e.g. the tibia and tarsus in *Acheta* and *Drosophila* or coxa and trochanter *in Periplaneta*) or disappear altogether as seems to be the case for small subsegments (the fifth tarsomere in *Drosophila*).

pathway, as a way of understanding the genetic basis for evolutionary changes in insect leg morphology.

Acknowledgments

We would like to thank Carl C. Freeman for his help with statistical analysis. We also thank Mizbauddin Mohiuddin for taking care of cricket cultures, Cassandra Extavour for providing helpful suggestions for in situ hybridization in *Acheta* embryos, Sarah Bishop for help with *Drosophila* experiments, Rose Phillips for help with *Periplaneta* work, and Jose I. Pueyo for help and suggestions with both. We also thank the anonymous reviewers whose comments significantly improved the manuscript. This work was supported by NIH grant GM071927 to A. P. and a Wayne State University Graduate Enhancement Research Fellowship to N. T., a Welcome Senior Fellowship to J. P. C. (ref. 087516), and a University of Sussex GTA studentship to J. C.

References

Abu-Shaar, M., Mann, R.S., 1998. Generation of multiple antagonistic domains along the proximodistal axis during *Drosophila* leg development. Development 125, 3821–3830.
Abzhanov, A., Kaufman, T.C., 2000. Homologs of *Drosophila* appendage genes in the patterning of arthropod limbs. Dev. Biol. 227, 673–689.
Angelini, D.R., Kaufman, T.C., 2004. Functional analyses in the hemipteran *Oncopeltus fasciatus* reveal conserved and derived aspects of appendage patterning in insects. Dev. Biol. 271, 306–321.
Averof, M., Patel, N.H., 1997. Crustacean appendage evolution associated with changes in Hox gene expression. Nature 388, 682–686.
Beermann, A., Jay, D.G., Beeman, R.W., Hulskamp, M., Tautz, D., Jurgens, G., 2001. The Short antennae gene of *Tribolium* is required for limb development and encodes the orthologue of the *Drosophila* Distal-less protein. Development 128, 287–297.
Bhat, K.M., Schedl, P., 1994. The *Drosophila* miti-mere gene, a member of the POU family, is required for the specification of the RP2/sibling lineage during neurogenesis. Development 120, 1483–1501.
Billin, A.N., Cockerill, K.A., Poole, S.J., 1991. Isolation of a family of *Drosophila* POU domain genes expressed in early development. Mech. Dev. 34, 75–84.
Bishop, S.A., Klein, T., Arias, A.M., Couso, J.P., 1999. Composite signalling from Serrate and Delta establishes leg segments in *Drosophila* through Notch. Development 126, 2993–3003.
Brown, S., DeCamillis, M., Gonzalez-Charneco, K., Denell, M., Beeman, R., Nie, W., Denell, R., 2000. Implications of the *Tribolium* Deformed mutant phenotype for the evolution of Hox gene function. Proc. Natl Acad. Sci. U. S. A. 97, 4510–4514.
Campbell, G., 2005. Regulation of gene expression in the distal region of the *Drosophila* leg by the Hox11 homolog, C15. Dev. Biol. 278, 607–618.
Casares, F., Mann, R.S., 2001. The ground state of the ventral appendage in *Drosophila*. Science 293, 1477–1480.
Chesebro, J., Hrycaj, S., Mahfooz, N., Popadić, A., 2009. Diverging functions of Scr between embryonic and post-embryonic development in a hemimetabolous insect, *Oncopeltus fasciatus*. Dev. Biol. 329, 142–151.
Cifuentes, F.J., Garcia-Bellido, A., 1997. Proximo-distal specification in the wing disc of *Drosophila* by the nubbin gene. Proc. Natl Acad. Sci. U. S. A. 94, 11405–11410.
Couso, J.P., Bishop, S.A., 1998. Proximo-distal development in the legs of *Drosophila*. Int. J. Dev. Biol. 42, 345–352.
Couso, J.P., Bishop, S.A., Martinez Arias, A., 1994. The wingless signalling pathway and the patterning of the wing margin in Drosophila. Development 120 (3), 621–636.
Damen, W.G., Saridaki, T., Averof, M., 2002. Diverse adaptations of an ancestral gill: a common evolutionary origin for wings, breathing organs, and spinnerets. Curr. Biol. 12, 1711–1716.

de Celis, J.F., Tyler, D.M., de Celis, J., Bray, S.J., 1998. Notch signalling mediates segmentation of the *Drosophila* leg. Development 125, 4617–4626.
Galindo, M.I., Bishop, S.A., Couso, J.P., 2005. Dynamic EGFR-Ras signalling in Drosophila leg development. Dev. Dyn. 233 (4), 1496–1508.
Gompel, N., Prud'homme, B., Wittkopp, P.J., Kassner, V.A., Carroll, S.B., 2005. Chance caught on the wing: cis-regulatory evolution and the origin of pigment patterns in *Drosophila*. Nature 433, 481–487.
Greenberg, L., Hatini, V., 2009. Essential roles for lines in mediating leg and antennal proximodistal patterning and generating a stable Notch signaling interface at segment borders. Dev. Biol. 330, 93–104.
Hrycaj, S., Mihajlovic, M., Mahfooz, N., Couso, J.P., Popadić, A., 2008. RNAi analysis of nubbin embryonic functions in a hemimetabolous insect, *Oncopeltus fasciatus*. Evol. Dev. 10, 705–716.
Hrycaj, S., Chesebro, J., Popadić, A., 2010. Functional analysis of Scr during embryonic and post-embryonic development in the cockroach, *Periplaneta americana*. Dev. Biol. 341, 324–334.
Inoue, Y., Mito, T., Miyawaki, K., Matsushima, K., Shinmyo, Y., Heanue, T.A., Mardon, G., Ohuchi, H., Noji, S., 2002. Correlation of expression patterns of homothorax, dachshund, and Distal-less with the proximodistal segmentation of the cricket leg bud. Mech. Dev. 113, 141–148.
Kango-Singh, M., Singh, A., Gopinathan, K.P., 2001. The wings of *Bombyx mori* develop from larval discs exhibiting an early differentiated state: a preliminary report. J. Biosci. 26, 167–177.
Lewis, E.B., 1978. A gene complex controlling segmentation in *Drosophila*. Nature 276, 565–570.
Lewis, D.L., DeCamillis, M., Bennett, R.L., 2000. Distinct roles of the homeotic genes Ubx and abd-A in beetle embryonic abdominal appendage development. Proc. Natl Acad. Sci. U. S. A. 97, 4504–4509.
Li, H., Popadić, A., 2004. Analysis of nubbin expression patterns in insects. Evol. Dev. 6, 310–324.
Mahfooz, N.S., Li, H., Popadić, A., 2004. Differential expression patterns of the hox gene are associated with differential growth of insect hind legs. Proc. Natl Acad. Sci. U. S. A. 101 (14), 4877–4882.
Mahfooz, N., Turchyn, N., Mihajlovic, M., Hrycaj, S., Popadić, A., 2007. Ubx regulates differential enlargement and diversification of insect hind legs. PLoS One 2, e866.
Mardon, G., Solomon, N.M., Rubin, G.M., 1994. dachshund encodes a nuclear protein required for normal eye and leg development in *Drosophila*. Development 120, 3473–3486.
Masumoto, M., Yaginuma, T., Niimi, T., 2009. Functional analysis of Ultrabithorax in the silkworm, *Bombyx mori*, using RNAi. Dev. Genes Evol. 219, 437–444.
Mirth, C., Akam, M., 2002. Joint development in the *Drosophila* leg: cell movements and cell populations. Dev. Biol. 246, 391–406.
Neumann, C.J., Cohen, S.M., 1998. Boundary formation in *Drosophila* wing: Notch activity attenuated by the POU protein Nubbin. Science 281, 409–413.
Ng, M., Diaz-Benjumea, F.J., Cohen, S.M., 1995. Nubbin encodes a POU-domain protein required for proximal–distal patterning in the *Drosophila* wing. Development 121, 589–599.
Panganiban, G., Sebring, A., Nagy, L., Carroll, S., 1995. The development of crustacean limbs and the evolution of arthropods. Science 270, 1363–1366.
Popadić, A., Panganiban, G., Rusch, D., Shear, W.A., Kaufman, T.C., 1998. Molecular evidence for the gnathobasic derivation of arthropod mandibles and for the appendicular origin of the labrum and other structures. Dev. Genes Evol. 208, 142–150.
Prpic, N.M., Damen, W.G., 2009. Notch-mediated segmentation of the appendages is a molecular phylotypic trait of the arthropods. Dev. Biol. 326, 262–271.
Prpic, N.M., Wigand, B., Damen, W.G., Klingler, M., 2001. Expression of dachshund in wild-type and Distal-less mutant *Tribolium* corroborates serial homologies in insect appendages. Dev. Genes Evol. 211, 467–477.
Prpic, N.M., Janssen, R., Wigand, B., Klingler, M., Damen, W.G., 2003. Gene expression in spider appendages reveals reversal of exd/hth spatial specificity, altered leg gap gene dynamics, and suggests divergent distal morphogen signaling. Dev. Biol. 264, 119–140.
Pueyo, J.I., Couso, J.P., 2005. Parallels between the proximal–distal development of vertebrate and arthropod appendages: homology without an ancestor? Curr. Opin. Genet. Dev. 15, 439–446.
Pueyo, J.I., Lanfear, R., Couso, J.P., 2008. Ancestral Notch-mediated segmentation revealed in the cockroach *Periplaneta americana*. Proc. Natl Acad. Sci. U. S. A. 105, 16614–16619.
Rauskolb, C., 2001. The establishment of segmentation in the *Drosophila* leg. Development 128, 4511–4521.
Rauskolb, C., Irvine, K.D., 1999. Notch-mediated segmentation and growth control of the *Drosophila* leg. Dev. Biol. 210, 339–350.
Rogers, B.T., Peterson, M.D., Kaufman, T.C., 2002. The development and evolution of insect mouthparts as revealed by the expression patterns of gnathocephalic genes. Evol. Dev. 4, 96–110.
Ronco, M., Uda, T., Mito, T., Minelli, A., Noji, S., Klingler, M., 2008. Antenna and all gnathal appendages are similarly transformed by homothorax knock-down in the cricket *Gryllus bimaculatus*. Dev. Biol. 313, 80–92.
Suzuki, Y., Squires, D.C., Riddiford, L.M., 2009. Larval leg integrity is maintained by Distal-less and is required for proper timing of metamorphosis in the flour beetle, *Tribolium castaneum*. Dev. Biol. 326, 60–67.
Tomoyasu, Y., Wheeler, S.R., Denell, R.E., 2005. Ultrabithorax is required for membranous wing identity in the beetle *Tribolium castaneum*. Nature 433, 643–647.
Tomoyasu, Y., Arakane, Y., Kramer, K.J., Denell, R.E., 2009. Repeated co-options of exoskeleton formation during wing-to-elytron evolution in beetles. Curr. Biol. 19, 2057–2065.
Wittkopp, P.J., Vaccaro, K., Carroll, S.B., 2002. Evolution of yellow gene regulation and pigmentation in *Drosophila*. Curr. Biol. 12, 1547–1556.
Wu, J., Cohen, S.M., 1999. Proximodistal axis formation in the *Drosophila* leg: subdivision into proximal and distal domains by Homothorax and Distal-less. Development 126, 109–117.
Yeo, S.L., Lloyd, A., Kozak, K., Dinh, A., Dick, T., Yang, X., Sakonju, S., Chia, W., 1995. On the functional overlap between two *Drosophila* POU homeo domain genes and the cell fate specification of a CNS neural precursor. Genes Dev. 9, 1223–1236.
Zhang, H., Shinmyo, Y., Mito, T., Miyawaki, K., Sarashina, I., Ohuchi, H., Noji, S., 2005. Expression patterns of the homeotic genes Scr, Antp, Ubx, and abd-A during embryogenesis of the cricket *Gryllus bimaculatus*. Gene Expr. Patterns 5, 491–502.